Supporting Information

Leung *et al.* 10.1073/pnas.0801232105

SI Text

WASP/Cdc42 fusions with FKBP/FRB show rapamycin-dependent activation of Arp2/3 complex. As a proof of principle that high concentrations of Cdc42(GDP) can override a weak affinity for WASP, we applied the well established FK506-Binding Protein (FKBP)-rapamycin system to Cdc42/WASP regulation (1). FKBP associates tightly with the FKBP-rapamycin binding (FRB) domain of the mammalian Target of Rapamycin protein (mTOR) only in the presence of the small molecule, rapamycin (K_D = 12 nM) (1, 2). Fusions of FKBP and FRB to a protein of interest can drive the conditional (rapamycin-mediated) colocalization and dimerization of proteins (1). In our studies, we used a modified Cdc42 construct lacking a C-terminal CAAX box and a minimal autoinhibited WASP construct containing only the GBD and VCA domains connected by a $(GGS)_2$ linker (referred to hereafter simply as WASP) (3). We generated four constructs in which Cdc42 and WASP were independently fused to either FKBP or FRB through glycine-serine linkers (Figs. S1 and S2, and Table S1). GST-pulldown assays showed that high-affinity binding of FKBP-Cdc42(GDP) to FRB-WASP or FKBP-WASP to FRB-Cdc42(GDP) occurred only in the presence of rapamycin (data not shown). Next, we examined the activity of these constructs toward Arp2/3 complex using a pyrene-actin assembly assay (Fig. S2). This assay is based on the increase in fluorescence of pyrene-labeled actin upon incorporation into filaments. Assembly of actin alone showed characteristic nucleation-dependent kinetics, with long lag phase and slow overall rate (Fig. S2, black curve). Arp2/3 complex alone has little effect on assembly kinetics (data not shown). When FKBP-Cdc42(GDP), FRB-WASP, and rapamycin are added together, WASP was activated toward Arp2/3 complex, as evidenced by a decreased lag time and increased actin assembly rate (Fig. S2, blue curve). This effect requires all three components, as all individual or pairwise combinations produced assembly kinetics identical to control. Actin assembly produced by the FKBP-Cdc42(GDP)/rapamycin combination was significantly below that of fully activated FRB-WASP (produced by addition of high concentrations of Cdc42(GDP); Fig. S2, compare green and blue curves). Nevertheless, this result showed that artificially enhanced association with Cdc42(GDP) could produce some relief of autoinhibition in WASP and consequent activation of Arp2/3 complex. The organization of the constructs was important, because assays with the opposite fusion pair, FKBP-WASP/FRB-Cdc42(GDP), showed no change in activity upon addition of rapamycin despite high affinity binding (data not shown). Rather than pursuing further optimization of the FKBP/FRB constructs to achieve higher rapamycin-dependent activity, we proceeded to explore whether the PhyB-Pif3 interaction could be used analogously to render the WASP/Cdc42(GDP) interaction light-dependent.

SI Methods

Generation of FKBP and FRB fusion proteins. FKBP residues 1–108 and TOR residues 2025–2114 comprising the FRB domain were fused to Cdc42 (residues 1–179, lacking the C-terminal CAAX box) or WASP (GBD-VCA; residues 230–310-GGSGGS-420–502) through a six residue linker composed of Gly and Ser residues (Table S1). FKBP fusions were subcloned into a modified pET15b vector (Novagen), containing an N-terminal His_6 tag followed by a TEV protease cleavage site. FRB fusions were subcloned into a modified pGEX-4T vector (GE Healthcare), containing an N-terminal GST (GST) tag followed by a TEV protease cleavage site. Fusion proteins were expressed in *E. coli* strain BL21(DE3) and purified using affinity and ion exchange chromatographies. Fusion proteins were cleaved with TEV protease, and the tag and protease were removed by subsequent Ni^{2+} or glutathione Sepharose affinity chromatography before a final gel filtration step.

1. Banaszynski LA, Wandless TJ (2006) Conditional control of protein function. *Chem Biol* 13:11–21.
2. Banaszynski LA, Liu CW, Wandless TJ (2005) Characterization of the FKBP. rapamycin. FRB ternary complex. *J Am Chem Soc* 127:4715–4721.
3. Leung DW, Rosen MK (2005) The nucleotide switch in Cdc42 modulates coupling between the GTPase-binding and allosteric equilibria of Wiskott-Aldrich syndrome protein. *Proc Natl Acad Sci USA* 102:5685–5690.

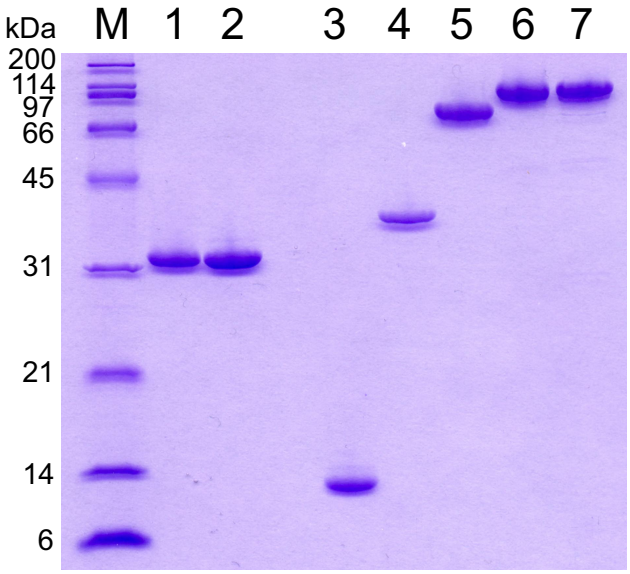

Fig. S1. Coomassie-stained SDS-PAGE of proteins used in this study show high purity. Lanes indicated are marked as follows: M, molecular weight markers; 1, FKBP-Cdc42; 2, FRB-WASP; 3, $Pif3_N$; 4, $Pif3_N$-WASP; 5, PhyB; 6, PhyB-Cdc42; 7, PhyB-WASP.

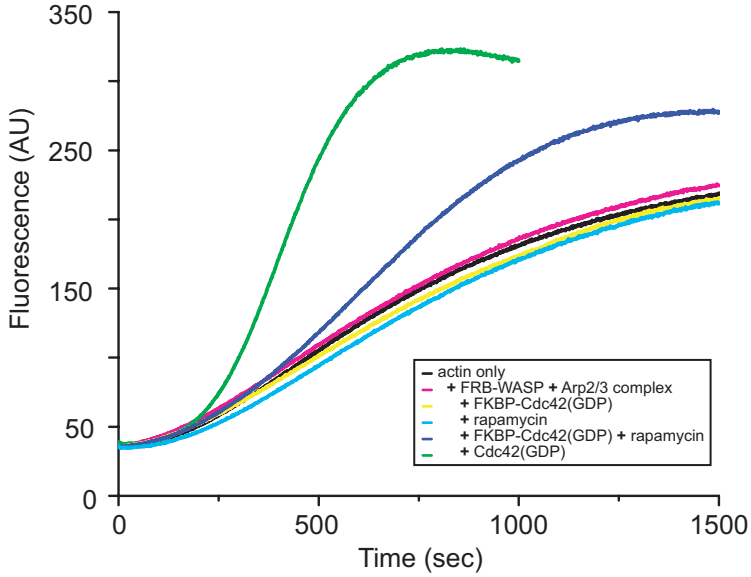

Fig. S2. FKBP-Cdc42(GDP) activates FRB-WASP only in the presence of rapamycin. Pyrene-actin assembly assays contained 4 μM actin (6% pyrene labeled), 10 nM Arp2/3 complex and 500 nM FRB-WASP (pink), except actin-only control (black). Assays additionally contained 500 nM FKBP-Cdc42(GDP) (yellow), 500 nM rapamycin (cyan), 500 nM FKBP-Cdc42(GDP) + 500 nM rapamycin 500 nM (blue), or 25 μM FKBP-Cdc42(GDP) (green).

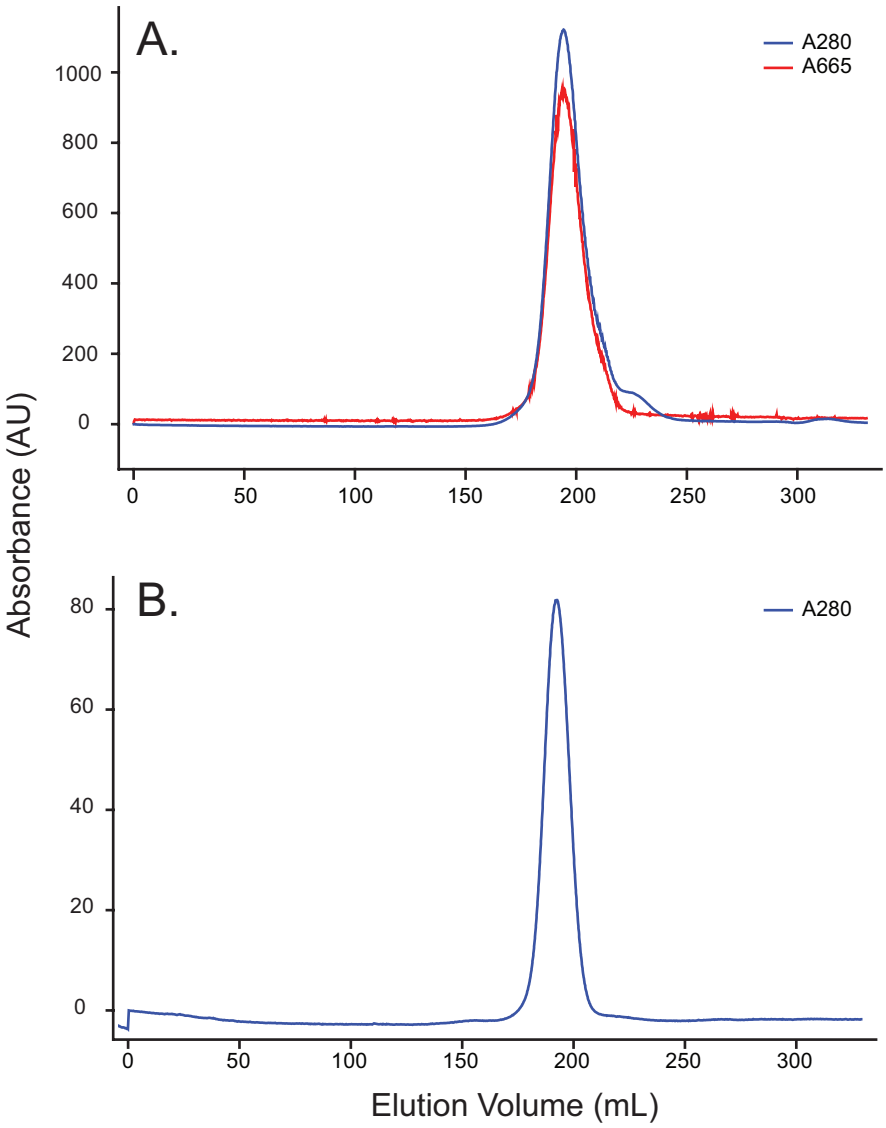

Fig. S3. Size exclusion chromatography of PhyB-WASP and $Pif3_N$. (*A*) PhyB-WASP elutes at ≈194 ml on a Superdex 200 26/60 column, corresponding to a calculated molecular mass of 89 kDa (actual mass = 89 kDa). (*B*) $Pif3_N$ elutes at ≈192 ml on a Superdex 75 26/60 column, corresponding to a calculated molecular mass of 22 kDa (actual mass = 11 kDa; NMR experiments indicate that $Pif3_N$ (1–100) is unfolded in solution (data not shown), accounting for its aberrant behavior in gel filtration chromatography).

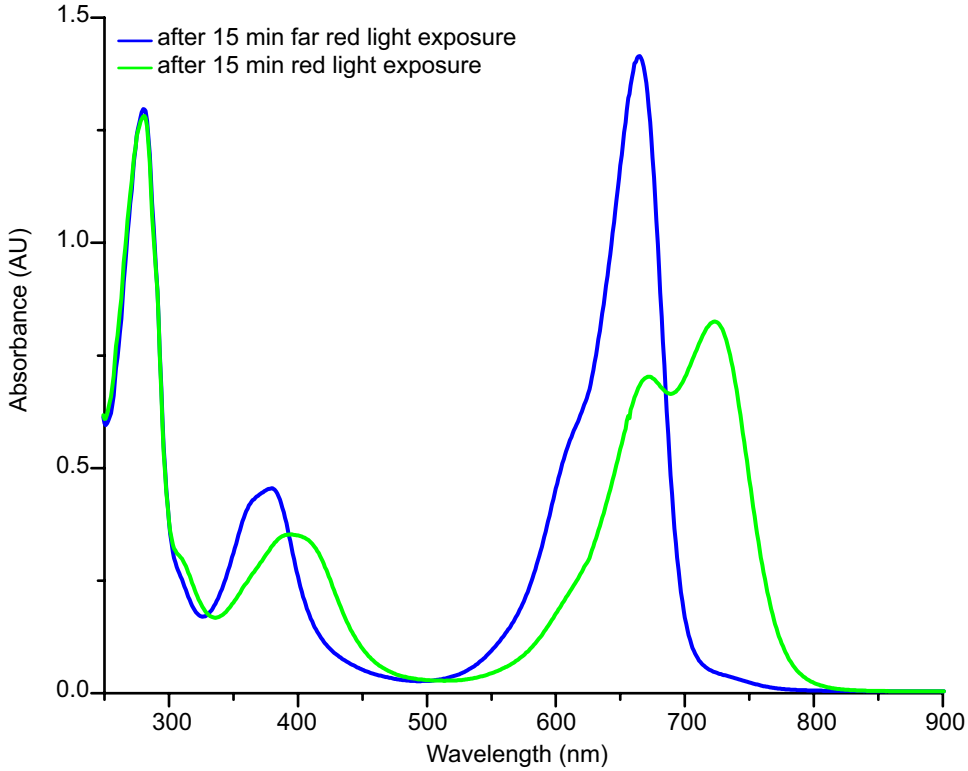

Fig. S4. Absorbance spectra of PhyB-WASP after irradiation with far red light (blue) and red light (green).

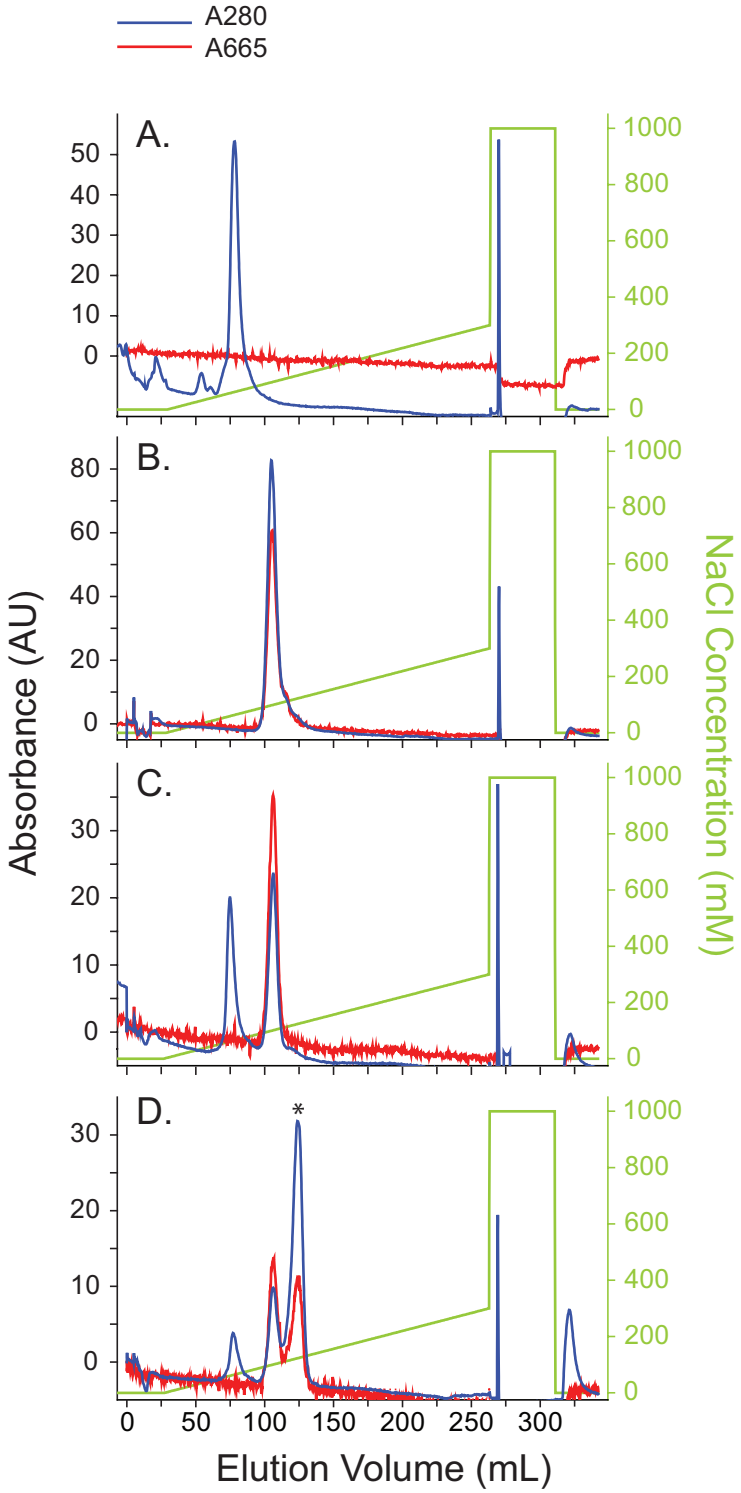

Fig. S5. PhyB-His binds Pif3$_N$ only after exposure to red light. (*A*) Pif3$_N$ eluted at ≈60 mM NaCl on an 8-ml Source 15Q 10/100 column. (*B*) PhyB-His, previously irradiated with 5 min far red light followed by 10 min red light, eluted at a ≈100 mM NaCl. (*C*) Pif3$_N$ and PhyB-His, mixed and then irradiated with far-red light for 5 min, eluted at similar NaCl concentrations as the individual components injected separately (in *A* and *B*). (*D*) PhyB-His and Pif3$_N$ form a complex (*) after 5 min far red irradiation followed by 10 min red light irradiation. The complex eluted at ≈120 mM NaCl. Chromatograms show protein absorbance at 280 nm (blue) and chromophore absorbance at 665 nm (red).

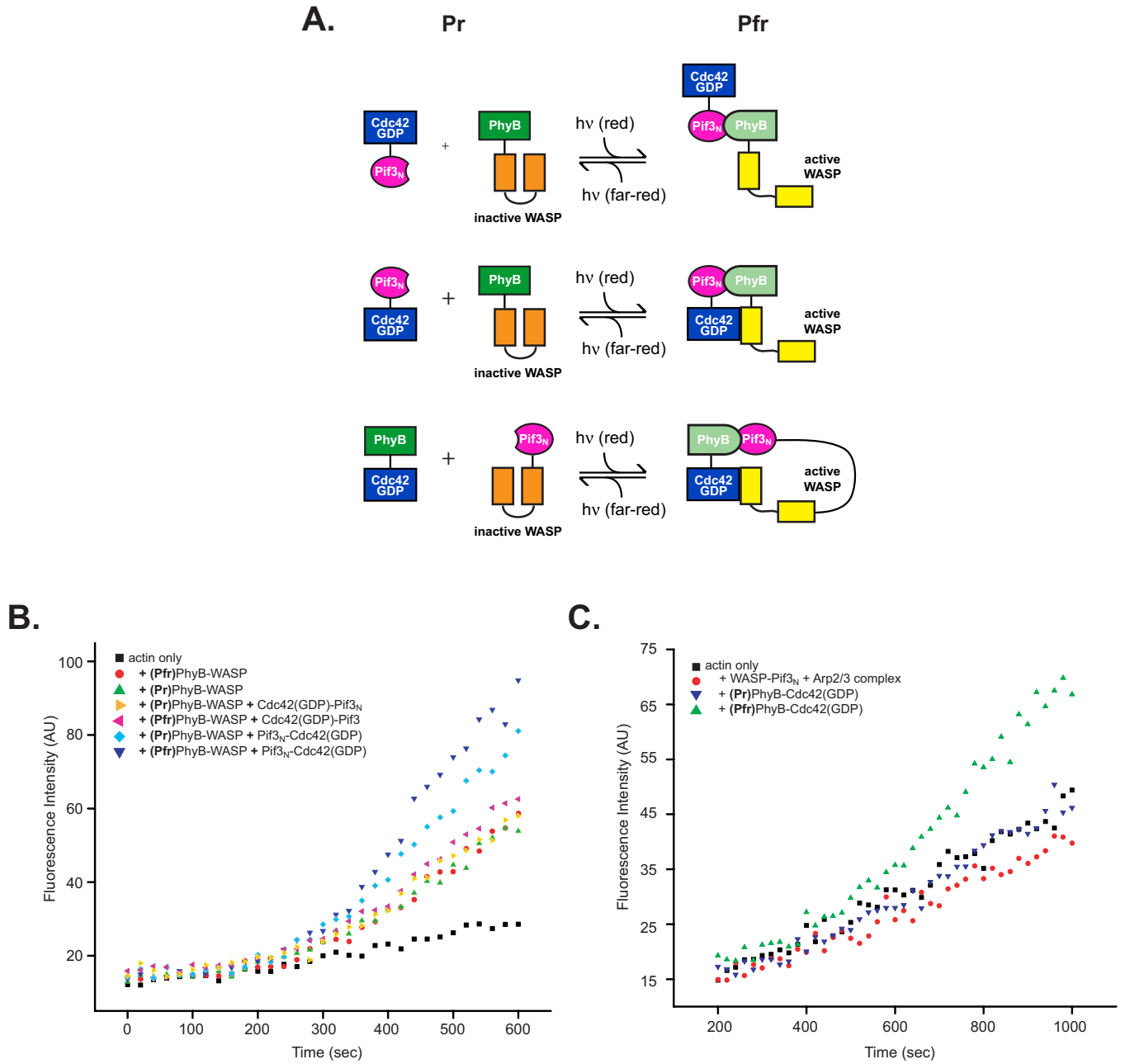

Fig. S6. Alternative domain organizations of PhyB and Pif3$_N$ fusions are not optimal for WASP activation. (*A*) Fusion constructs and combinations tested (compare with Fig. 4). (*B*) Pyrene-actin assembly assays contained 4 μM actin (6% pyrene-labeled), 10 nM Arp2/3 complex (except actin-only control (black squares)) plus 125 nM either Pfr (red circles) or Pr (green triangles) PhyB-WASP. Assays additionally contained 500 nM Cdc42(GDP)-Pif3$_N$ (Pr = orange triangles; Pfr = red triangles) or 1 μM Pif3$_N$-Cdc42(GDP) (Pr = cyan diamonds; Pfr = blue inverted triangles). (*C*) Assays performed as in (*B*), but with 250 nM WASP-Pif3$_N$ (red circles) plus either 1.5 μM (Pr)PhyB-Cdc42(GDP) (inverted blue triangles) or 1.5 μM (Pfr)PhyB-Cdc42(GDP) (green triangles).

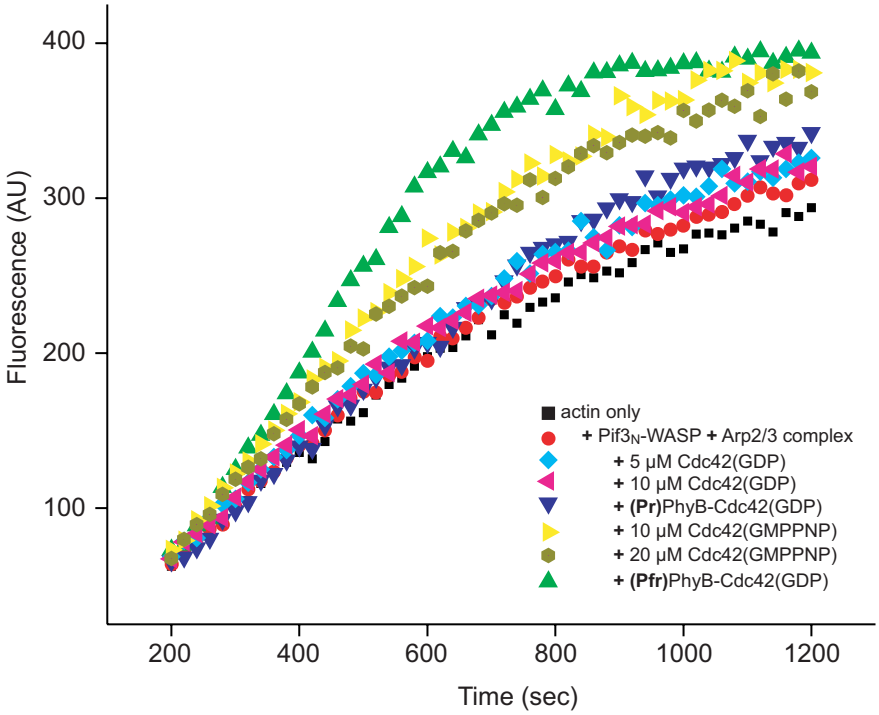

Fig. S7. Light-dependent activation of $Pif3_N$-WASP by PhyB-Cdc42(GDP). Actin assembly assays were performed as in Fig. 4, but with an actin preparation with lower baseline assembly rate (probably due to more efficient removal of short filaments during purification). Note that assembly induced by (Pfr)PhyB-Cdc42(GDP) was the same as in Fig. 4*A*, but that induced by (Pr)PhyB-Cdc42(GDP) was appreciably less, because of the lower baseline rate of actin alone. Thus, in these experiments the magnitude of functional switching between the Pfr and Pr states was larger than in Fig. 4*A*.

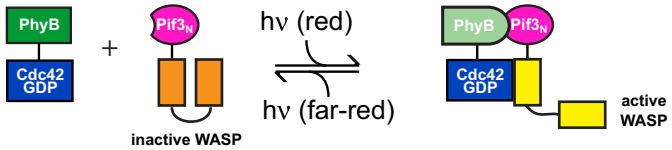

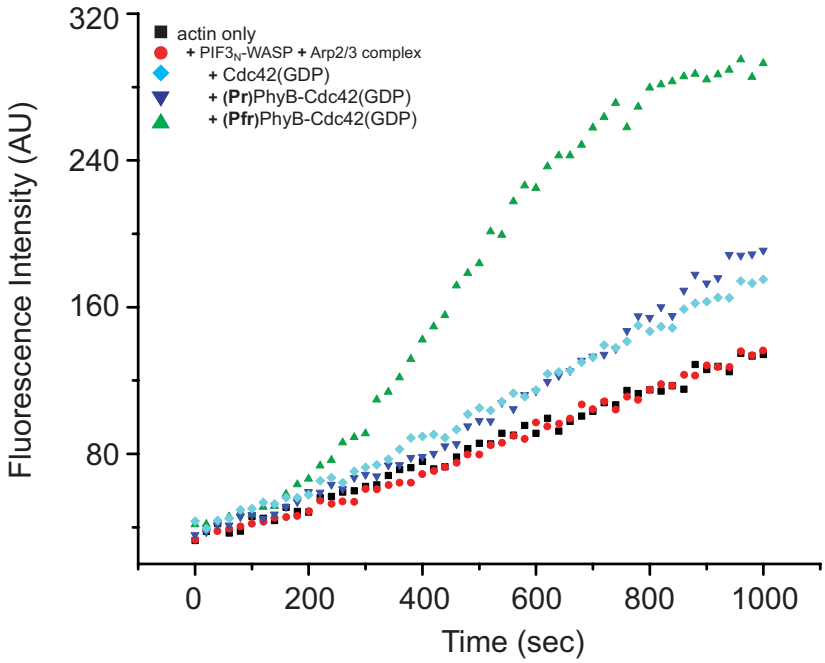

Fig. S8. (Pfr)PhyB-Cdc42(GDP) is a better activator of $Pif3_N$-WASP than Cdc42(GDP) or Cdc42(GMPPNP). Pyrene-actin polymerization assays of $Pif3_N$-WASP were performed in the absence and presence of Cdc42(GDP) or Cdc42(GMPPNP) at two different concentrations. Assays of $Pif3_N$-WASP in the presence of (Pfr)PhyB-Cdc42(GDP) or (Pr)PhyB-Cdc42(GDP) are shown for comparison (identical data shown in Fig. 4*A*).

Table S1. Constructs used in this work

Construct	Amino acid sequence*
FKBP/FRB constructs	
FKBP-Cdc42	*NdeI*-FKBP(1–108)-GGSGGS-Cdc42(1–179)-*BamHI*
FRB-WASP	*NdeI*-mTOR(2025–2114)-GSGGSG-WASP(230–310-GGSGGS-420–501)-*BamHI*
FKBP-WASP	*NdeI*-FKBP(1–108)-GSGGSG-WASP(230–310-GGSGGS-420–501)-*BamHI*
FRB-Cdc42	*NdeI*-mTOR(2025–2114)-GGSGGS-Cdc42(1–179)-*BamHI*
PhyB†/Pif3 constructs	
PhyB	*NdeI*-PhyB(1–651)-*NotI*
$Pif3_N$	*NdeI*-Pif3(1–100)-*NotI*
PhyB-Cdc42	*NdeI*-PhyB(1–651)-*NotI*-GSGGSGGSGGSGGSGGSGGS-*KpnI*-Cdc42(1–179)-*BamHI*
$Pif3_N$-WASP	*NdeI*-Pif3(1–100)-*NotI*- GSGGSGGSGGSGGSGGSGGS-*KpnI*-WASP(230–310-GGSGGS-420–501)-*BamHI*
PhyB-WASP	*NdeI*-PhyB(1–651)-*NotI*-GSGGSGGSGGSGGSGGSGGS-*KpnI*- WASP(230–310-GGSGGS-420–501)-*BamHI*
$Pif3_N$-Cdc42	*NdeI*-Pif3(1–100)-*NotI*- GSGGSGGSGGSGGSGGSGGS-*KpnI*- Cdc42(1–179)-*BamHI*
WASP-$Pif3_N$	*NdeI*- WASP(230–310-GGSGGS-420–501)- *NotI*-GSGGSGGSGGSGGSGGSGGS-*KpnI*- Pif3(1–100)-*NotI*
Cdc42-$Pif3_N$	*NdeI*- Cdc42(1–179)-*NotI*- GSGGSGGSGGSGGSGGSGGS-*KpnI*- Pif3(1–100)-*NotI*
WASP-PhyB	*NdeI*- WASP(230–310-GGSGGS-420–501)- *NotI*-GSGGSGGSGGSGGSGGSGGS-*KpnI*- PhyB(1–651)-*NotI*
Cdc42-PhyB	*NdeI*- Cdc42(1–179)-*NotI*- GSGGSGGSGGSGGSGGSGGS-*KpnI*- PhyB(1–651)-*NotI*

*Restrictions sites in the amino acid sequence that are used for subcloning purposes are italicized.
†A silent mutation was introduced to eliminate an internal BamHI restriction site in the wildtype PhyB(1–651) sequence.